Microsecond Rotational Dynamics of Spin-Labeled Myosin Regulatory Light Chain Induced by Relaxation and Contraction of Scallop Muscle†

Osha Roopnarine,‡ Andrew G. Szent-Györgyi,§ and David D. Thomas*,‡

Department of Biochemistry, University of Minnesota Medical School, Minneapolis, Minnesota 55455, and Department of Biology, Brandeis University, Waltham, Massachusetts 02154

Received April 14, 1998; Revised Manuscript Received July 27, 1998

ABSTRACT: We have used saturation transfer electron paramagnetic resonance (ST-EPR) to study the rotational dynamics of spin-labeled regulatory light chain (RLC) in scallop (*Placopecten magellanicus*) muscle fibers. The single cysteine (Cys 51) in isolated clam (*Mercenaria*) RLC was labeled with an indanedione spin label (InVSL). RLC was completely and specifically extracted from scallop striated muscle fibers, eliminating the Ca sensitivity of ATPase activity and isometric force, which were both completely restored by stoichiometric incorporation of labeled RLC. The EPR spectrum of the isolated RLC revealed nanosecond rotational motions within the RLC, which were completely eliminated when the labeled RLC was bound to myosin heads in myofibrils or fibers in rigor. This is the most strongly immobilized RLC-bound probe reported to date and thus offers the most reliable detection of the overall rotational motion of the LC domain. Conventional EPR spectra of oriented fibers indicated essentially complete probe disorder, independent of ATP and Ca, eliminating orientational dependence and thus making this probe ideal for unambiguous measurement of microsecond rotational motions of the LC domain by ST-EPR. ST-EPR spectra of fibers in rigor indicated an effective rotational correlation time (τ_r^{eff}) of 140 ± 5 μs, similar to that observed for the same spin label bound to the catalytic domain. Relaxation by ATP induced microsecond rotational motion (τ_r^{eff} = 70 ± 4 μs), and this motion was slightly slower upon Ca activation of isometric contraction (τ_r^{eff} = 100 ± 5 μs). These motions in relaxation and contraction are similar to, but slower than, the motions previously reported for the same spin label bound to the catalytic domain. These results support a model for force generation involving rotational motion of the LC domain relative to the catalytic domain and dynamic disorder-to-order transitions in both domains.

While muscle contraction models have long proposed a force-generating transition between two distinct axial orientations of the myosin head on actin (*1*), EPR[1] studies with probes attached to the catalytic ("motor") domain of myosin in contracting muscle fibers have shown no evidence for a unique axial head orientation that is distinct from that of rigor (no ATP) (*2*, *3*). Rather than a transition between two angles, the EPR studies indicated a transition from dynamic disorder to order in the catalytic domain upon contraction (*2*−*7*). This could be enough to explain how force is generated, but attention has also been focused on models in which the myosin head is segmentally flexible, such that the light-chain (LC) domain rotates relative to the catalytic domain (*8*−*10*). A test of this hypothesis is best accomplished by using spectroscopic probes directed specifically to the LC domain.

Molluscan and vertebrate striated muscle myosins have two LCs associated noncovalently with each head; these are usually termed the essential and regulatory light chains (ELC and RLC), based primarily on their functional roles in molluscan muscle. Crystal structures of chicken skeletal S1 (*11*) and the LC domain of scallop S1 (*12*) show that both light chains wrap around the long α-helical C-terminal end of the S1 heavy chain. Molluscan striated muscle is regulated by direct Ca binding to domain I of the ELC, which requires specific interactions with residues of the heavy chain and RLC (*12*−*15*). The RLC also plays a crucial functional role in scallop muscle regulation in that it inhibits the myosin ATPase activity in the absence of Ca (*16*). However, removal of the divalent cation in RLC disrupts the apolar interaction between the heavy and light chains and results

† This work was supported by grants to D.D.T. (NIH AR32961, Muscular Dystrophy Association, and Minnesota Supercomputer Institute) and A.G.S.-G. (NIH AR15963, NIH AR41803, and Muscular Dystrophy Association).

* To whom correspondence should be addressed. E-mail ddt@ddt.biochem.umn.edu.

‡ University of Minnesota. E-mail osha@ddt.biochem.umn.edu.

§ Brandeis University. E-mail szentgyorgyi@binah.cc.brandeis.edu.

[1] Abbreviations: EPR, electron paramagnetic resonance; ATP, adenosine triphosphate; CP, creatine phosphate; CPK, creatine phosphokinase; DTT, dithiothreitol; DTNB, 5,5′-dithiobis(2-nitrobenzoic acid); EGTA, ethyleneglycol bis(β-aminoethyl ether)-*N*,*N*,*N*′,*N*′-tetraacetic acid; EDTA, ethylenediaminetetraacetic acid; MOPS, 3-(*N*-morpholino)propanesulfonic acid; P_i, inorganic phosphate; PMSF, phenylmethanesulfonyl fluoride; S1, myosin subfragment 1; SH1 (Cys 707), most reactive sulfhydryl group in myosin head; ELC, essential light chain; LC, light chain; RLC, regulatory light chain; TM, tropomyosin; FDNA, 3-(5-fluoro-2,4-dinitroanilino)-2,2,5,5-tetramethyl-1-pyrrolidinyloxy; IASL, 2,2,6,6-tetramethyl-4-piperidinyl)iodoacetamide; InVSL, 2-[-oxyl-2,2,5,5-tetramethyl-3-pyrrolin-3-yl)methenyl]-indane-1,3-dione; MSL, *N*-(1-oxy-2,2,6,6-tetramethyl-4-piperidinyl)maleimide; ST-EPR, saturation transfer EPR; G, gauss; TE_{102} cavity, transverse electric cavity; $2T_{\parallel}'$, splitting between the outer extrema of conventional EPR spectrum; τ_r^{eff}, effective rotational correlation time; L''/L, line height ratio in low field region of ST-EPR spectrum.

S0006-2960(98)00836-8 CCC: $15.00
Published on Web 09/25/1998

in dissociation of the RLC (*12*, *14*). The Ca sensitivity of the actin-activated myosin ATPase and force-generating ability are lost when RLC is removed from scallop myosin heads in solution (*16*, *17*, *43*) or in muscle fibers (*18*). Restoration of Ca-dependent myosin function is achieved by rebinding RLC from any regulated myosin source, e.g., clam (*Mercenaria*) or chicken gizzard RLC (*19*). Both RLC removal and functional reincorporation can be accomplished completely under mild conditions and verified by a sensitive functional assay of calcium-sensitive ATPase or force (*18)*. In skeletal muscle, RLC extraction requires harsher conditions and is less complete, reincorporation is less specific, the functional effects of light chains are more subtle, and their physiological significance is less clear. In skeletal muscle, the RLC does not inhibit the myosin ATPase. RLC depletion or phosphorylation in skeletal muscle fibers causes a small shift in the Ca dependence of contraction, suggesting that RLC may be involved in modulating the calcium sensitivity of cross-bridge cycling (*20*). Removal of either or both light chains (ELC or RLC) decreases the motility of actin filaments on myosin fragments but does not affect the actin-activated ATPase activity (*21*), suggesting that the LC/heavy chain interaction is essential for normal movement.

Previous studies with spectroscopic probes on the RLC of rabbit skeletal muscle fibers have not been conclusive. In these studies, considerable probe disorder was present, two distinct probe angles were not resolved, and little or no orientational change was detected upon contraction (*6*, *22*−*25*). Much more clear results were obtained with scallop muscle, in which a spin label on Cys 108 of gizzard RLC reported a 36° rotation of the LC domain in the transition from relaxation to contraction (*26*). This is the first clear evidence for a distinct angular myosin transition in muscle.

Although the orientational properties of the RLC domain have been studied, the rotational motions of the LC domain during force generation are unknown. This is primarily because of the limitations of the spin-labeled LC. An important requirement for studying the global rotation of a protein is that the probe should be rigidly immobilized on the protein (*27*). All of the previous spin probes (maleimide or iodoacetamide) were weakly immobilized on the RLC on the myosin head and therefore not suitable for ST-EPR experiments (*22*, *23*, *28*). We previously reported on an indanedione spin label, designated InVSL, that is strongly immobilized on RLC exchanged into scallop fibers in rigor (*29*, *30*). We determined that the spin label on scallop fibers with InVSL-RLC had no orientational dependence, making it ideal for studying the rotational dynamics by ST-EPR spectroscopy.

Therefore, we have labeled *Mercenaria* RLC with InVSL to study the rotational dynamics of the LC domain of scallop fibers using ST-EPR spectroscopy. We used *Placopecten magellanicus* striated scallop fibers because >95% RLC extraction and reincorporation could be achieved and characterized by both ATPase and mechanical assays (*18)*. The advantages of using *Mercenaria* RLC are that (a) it has a single cysteine (Cys 51) that allows specific labeling (*31*), (b) it restores Ca-sensitive myofibrillar ATPase activity in RLC-extracted scallop fibers (*19*), (c) Cys 51 is ideally located for measuring global rotation, since the crystal structure of the LC domain suggests that this residue is well buried (*12*), and (d) Cys 51 is distal from the specific Ca binding site. The latter may allow the spin label to be independent of local conformational changes due to Ca binding. We report on the rotational dynamics of RLC-labeled myosin heads in rigor, relaxation, and contraction.

MATERIALS AND METHODS

Reagents and Solutions. The spin label, InVSL, was synthesized as described by Hankovszky et al. (*32*) and provided by Dr. Kálmán Hideg, University of Hungary, Pécs. CPK and DTT were obtained from Boehringer Mannheim Biochemicals (Indianapolis, IN). ATP and CP and other reagents were obtained from Sigma (St Louis, MO). The following solutions (*33*, *34*) were used for RLC in solution: guanidine reducing solution: 6 M guanidine hydrochloride, 10 mM DTT, and 10 mM MOPS (pH 7.0); NaP_i buffer: 25 mM NaCl, 5 mM $NaPO_4$ (pH 6.0), and 3 mM NaN_3; NaN_3 wash: 40 mM NaCl, 5 mM $NaPO_4$ (pH 7.0), and 0.1 mM NaN_3; $MgCl_2$ wash: NaN_3 wash plus 2 mM $MgCl_2$; EDTA wash: $MgCl_2$, wash plus 1 mM EDTA. The following solutions were used for preparation of scallop muscle fiber bundles: Ringer's solution: 440 mM NaCl, 10 mM KCl, 4 mM $MgSO_4$, 40 mM $MgCl_2$, 10 mM imidazole (pH 7.0), 0.1 mM NaN_3, and 0.05% PMSF; rigor solution: 50 mM KCl, 5 mM $MgCl_2$, 5 mM EGTA, 20 mM imidazole (pH 7.0) and 0.1 mM NaN_3; chemical skinning solution: 0.5% Triton X-100, 50 mM KCl, 5 mM EGTA, 5 mM $MgCl_2$, 5 mM ATP, 20 mM imidazole (pH 7.0), and 0.1 mM NaN_3; extraction solution: NaN_3 wash plus 15 mM EDTA; myofibril wash: 20 mM KCl, 1 mM $MgCl_2$, 10 mM MOPS (pH 7.0), and 0.1 mM EGTA. The solutions used for scallop fiber bundles in EPR experiments were rigor solution, relaxation solution with an ATP regenerating solution, and contraction solution and were described previously by Roopnarine and Thomas (*3*). All preparations and labeling procedures were performed at 4 °C.

Preparations and Assays. Mercenaria RLC were prepared as described previously (*28*). *Placopecten magellanicus* scallops were obtained from Woods Hole, MA, and kept alive in an aerated seawater tank at 4 °C. The scallop muscle was dissected and prepared at 4 °C as described by Simmons and Szent-Györgyi (*33*, *34*) and was used within 2−3 days because storage in glycerol abolishes the mechanical and contractile properties of the muscle fibers (*34*). Fiber bundles (≈0.5 mm in diameter) were dissected and tied on wooden sticks and stored in Ringer's solution at 4 °C. The sarcoplasmic membranes were permeabilized by chemically skinning the fibers essentially as described by Simmons and Szent-Györgyi (*33*, *34*), except that it was done for 2 h at 4 °C.

The LC content in scallop myofibrils was determined on a 12.5% acrylamide gel in 8 M urea (*17*). A Hoefer GS-300 scanning densitometer interfaced with Hoefer GS-365 software for an IBM-compatible computer was used to quantitate the LCs on the urea gels. Mg-ATPase assays in the presence (MgATPase + Ca) and absence (MgATPase − Ca) of Ca were done with similar solutions as described by Simmons and Szent-Györgyi (*34*) at 25 and 11 ± 1 °C. For the MgATPase − Ca assay, the solution was 20 mM KCl, 1 mM $MgCl_2$, 0.75 mM ATP, 1.5 mM EGTA, and 10 mM MOPS (pH 7.5), and for the MgATPase + Ca assay,

the solution was the same as the MgATPase − Ca solution except that 3 mM $CaCl_2$ was used. The ATPase assay was measured as described by Roopnarine et al. (*27*) and the ATPase activity was reported in micromoles of P_i per milligram per minute. Calcium sensitivity of myofibril samples is defined as [1 − (MgATPase − Ca/MgATPase + Ca)] × 100. Isometric tension of scallop fiber bundles was measured essentially as described previously (*33*, *34*).

Preparation of Labeled Proteins. Lyophilized *Mercenaria* RLC was thiol-reduced in guanidine reducing solution for 1 h at room temperature and then dialyzed extensively against NaP_i buffer (pH 6.5) in a vertical Hoefer dialysis apparatus to remove excess guanidine. The number of free cysteines in *Mercenaria* RLC was determined by DTNB titration at pH 8.0 (*35*). Immediately before labeling, the pH of the RLC solution was increased to 8.0 by addition of an appropriate amount of 0.5 M dibasic sodium phosphate. The reaction with InVSL (2:1 ratio of spin label to free cysteine) was initiated after 5 min, and the reaction mixture was gently stirred at 4 °C for 3 h. The labeling procedure was optimum after 3 h as determined by monitoring the appearance of an immobilized EPR signal during the labeling reaction as described by Roopnarine et al. (*27*). The reaction mixture was diluted 3-fold into NaN_3 wash (pH 7.0) and then concentrated in Amicon Centricon units (molecular weight cutoff = 10 000) by centrifuging at 5000*g*. This was repeated at least 4 times to remove unreacted spin label, and then the sample was dialyzed against $MgCl_2$ wash buffer (pH 7.0) overnight at 4 °C.

RLC Incorporation in Myofibrils, Glass Beads, and Muscle Fibers. Scallop myofibrils were prepared and RLC was extracted and reincorporated as described by Chantler and Szent-Györgyi (*16*). Labeled RLC was covalently attached to glass beads as described by Roopnarine et al. (*27*). The scallop RLC was removed from the scallop muscle bundles using several modifications of the procedure described by Simmons and Szent-Györgyi (*34*) for thin scallop muscle fiber bundles. Both the temperature and incubation time for RLC extraction from scallop fiber bundles were varied. The muscle fiber bundles were tied at both ends with silk surgical threads and gently pulled into 100 μL glass capillaries and held isometrically with Tygon tubing connected to a peristaltic pump. The bundles were washed with NaN_3 wash equilibrated at 10, 20, 22, and 25 °C for 5 min (flow rate = 2.0 mL/min), then with NaN_3 wash containing 15 mM EDTA for different time intervals, and finally in NaN_3 wash for 5 min. The fiber bundle was blotted dry, minced, and dissolved in urea electrophoresis sample buffer at room temperature for 30 min and the RLC/ELC content was determined from a urea gel by densitometry (*17*). We determined that optimal condition for >95% RLC depletion without irreversible damage to the fiber myofibril ATPase and mechanical property was a 2 h incubation at 24 ± 1 °C.

After RLC extraction, the fiber bundles were washed with NaN_3 wash at room temperature for 5 min and then in $MgCl_2$ wash for 10 min at 4 °C and kept on ice. InVSL-labeled or unlabeled *Mercenaria* RLC (3−4 mg/mL) in $MgCl_2$ wash was flowed into the capillaries containing the fiber bundles and incubated on ice overnight. The RLC solution was removed and the fiber bundles were washed with $MgCl_2$ wash (three times) to remove unbound RLC and were then immediately used for EPR experiments, ATPase assays, and tension measurements.

EPR Spectroscopy. Conventional EPR spectra (first harmonic absorption in-phase) were acquired with a model ESP 300 spectrometer (Bruker Instruments, Billerica, MA) as described by Roopnarine et al. (*27*). EPR spectra of oriented muscle fibers were acquired with a TM_{110} cavity that was modified to hold a capillary parallel to the magnetic field (*3*, *36*, *37*). ST-EPR spectra of muscle fibers were acquired in a TE_{102} cavity as described by Roopnarine et al. (*27*) and Roopnarine and Thomas (*3*) at 11 ± 2 °C while buffer solutions were perfused with a peristaltic pump.

Spectroscopic Data Analysis. Each spectrum was baseline-corrected and normalized to unit spin concentration as described by Roopnarine and Thomas (*37*). Each spectrum in this paper is plotted with a 100 G baseline. The number of spin labels in the labeled RLC was determined by comparison of the double integrals of the spectra for labeled RLC and 0.1 mM InVSL in the same solution. This was compared with molar concentration of the labeled RLC to yield the spin label:RLC ratio of 0.8−1.0. The effective rotational correlation time (τ_r^{eff}) for spin-labeled RLC was determined from the conventional EPR spectrum using eq 1, assuming isotropic rotational diffusion (*38*, *39*).

$$\tau_r = a(1 - T'_{||}/T_{||})^b \quad (1)$$

where $2T_{||}'$ and $2T_{||}$ are the splittings between the outer extrema of the experimental spectrum and a rigid limit spectrum, respectively (illustrated below in Figure 2). The rigid limit spectrum ($2T_{||} = 71.6 \pm 0.1$ G) was obtained from labeled RLC immobilized on glass beads. The values for parameters were $a = 5.4 \times 10^{-10}$ s and $b = -1.36$.

ST-EPR spectra were normalized and analyzed to determine effective rotational correlation times in the microsecond time range, using the line height parameter L''/L (*40*), using an empirical calibration plot obtained with InVSL undergoing isotropic rotational motions (*27*). The restriction in the angular amplitude of motion was analyzed as described by Howard et al. (*41*). The contraction spectrum was also analyzed by fitting it to a linear combination of two endpoint spectra (obtained in rigor and relaxation) as described previously (*3*), using

$$\text{contraction} = X_{RIG}\text{rigor} + (1 - X_{RIG})\text{relaxation} \quad (2)$$

where X_{RIG} is the mole fraction of the rigor spectrum, which was varied while χ^2 was minimized between the composite and experimental spectra.

RESULTS

Characterization of RLC-Labeled Fibers. Densitometric analysis of urea gels (Figure 1) showed that control (chemically skinned) scallop myofibrils typically had a RLC/ELC ratio of 0.90 ± 0.05 (Figure 1, lane 1). RLC extraction in 15 mM EDTA (in NaN_3 wash) decreased the ratio to 0.10 ± 0.05 (Figure 1, lane 2), and reincorporation of either unlabeled (data not shown) or labeled RLC restored the ratio to 0.9 ± 0.05 (Figure 1, lane 3; Table 1, column 1). The extraction procedure did not affect the ELC content of the fiber bundles (Figure 1). Functional incorporation of unlabeled or labeled RLC was determined from myofibrillar

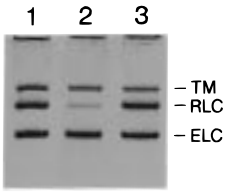

FIGURE 1: Urea−PAGE of scallop myofibrils: Lane 1, chemically skinned; lane 2, RLC extracted; lane 3, reincorporated with InVSL-labeled *Mercenaria* RLC.

Table 1: RLC Content and MgATPase Activity of Myofibrils Prepared from Scallop Fibers[a]

myofibrils	RLC/ELC	MgATPase (−Ca)	MgATPase (+Ca)	(%) Ca sensitivity
control	0.90 ± 0.05	0.02 ± 0.005	0.87 ± 0.05	97.7 ± 1
RLC extracted	0.10 ± 0.05	0.25 ± 0.02	0.32 ± 0.02	22.0 ± 0.05
reincorporated with labeled RLC	0.90 ± 0.05	0.03 ± 0.005	0.86 ± 0.05	96.5 ± 1

[a] The RLC/ELC ratios were determined from densitometric analysis of urea−acrylamide gels. The ATPase assays were done at 25 °C and are reported in micromoles of inorganic phosphate per milligram per minute. Ca sensitivity of myofibril samples is defined as the percentage decrease in activity due to the removal of Ca. Reported values are the mean ± SEM for $n = 4$.

MgATPase assays (±Ca) and isometric tension measurements of fiber bundles. The ATPase activity of control scallop myofibrils at 25 °C in the presence of Ca was 0.87 ± 0.05 μmol of P_i mg^{-1} min^{-1}, which is about 40 times higher than that observed in the absence of Ca (Table 1, row 1). RLC extraction resulted in a 12-fold activation of MgATPase − Ca activity (Table 1, row 2), indicating a loss of Ca sensitivity. Reincorporation of *Mercenaria* RLC restored the MgATPase activities to near normal values (Table 1, row 3). There is a direct relationship between the RLC content (measured from urea−acrylamide gels, Figure 1) and the Ca sensitivity of ATPase activity (Table 1, columns 1 and 4).

Because the mechanical properties of scallop fibers deteriorate rapidly at room temperature, EPR experiments were done at 11 °C, which is the natural temperature for *Placopecten magellanicus* scallops. MgATPase + Ca values at 11° C were 55% less than at 25 °C, with no change in Ca sensitivity, as previously shown (*16*). Extraction of native scallop RLC from the fiber bundles resulted in an 85% ± 0.5% decrease in the active isometric tension of control fiber bundles (1−2.5 N/cm^2). This is consistent with the fraction of RLC extracted, as determined from densitometry analysis of urea gels (0.90 ± 0.05) (Table 1, column 5). Reincorporation with either unlabeled or labeled RLC restored the active tension values to within 5% of original tension values. It was previously shown that the mechanical function of scallop striated muscle fibers deteriorates within days after the animal is sacrificed (*34*). In addition, MgATPase assays have shown that incomplete reincorporation of RLC causes myosin heads to remain in an activated state. To ensure that the fiber bundles used in the EPR experiments were active, we checked for unloaded shortening in both relaxation and contraction solutions after acquisition of the EPR spectra. Fiber bundles that had incomplete RLC reincorporation (determined from urea gels) shortened in both relaxation and contraction solutions, indicating loss of Ca sensitivity. Data were included in statistical analysis only for fibers that shortened in contraction solution but not in relaxation solution and only for fibers that returned to the original rigor EPR spectrum after removal of ATP and Ca at the end of the EPR experiment.

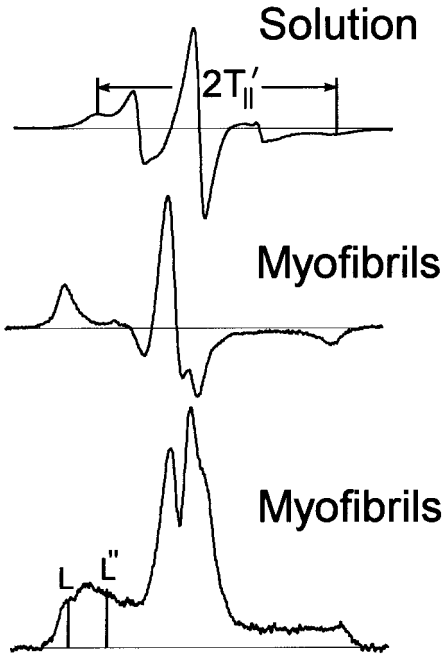

FIGURE 2: Conventional (top and middle) and ST-EPR (bottom) spectra of InVSL-RLC in solution (NaN_3 wash) (top) and on myofibrils in rigor solution (middle and bottom). Spectral parameters $2T_{\parallel}'$ and L''/L, used to analyze conventional and ST-EPR spectra, respectively, are illustrated. Each spectrum has been normalized to unit concentration before plotting.

EPR Spectra of Labeled RLC. We labeled 0.8−1.0 cysteine/mol of RLC. The conventional EPR spectrum of labeled RLC in solution (Figure 2, top) showed two components, one with a narrow splitting (weakly immobilized) and another with a broader splitting (strongly immobilized). The splitting between the outer extrema ($2T_{\parallel}'$, illustrated in Figure 2) of the latter component in the absence of divalent cation was 62.6 ± 0.1 G, corresponding to an effective rotational correlation time of 9 ± 0.2 ns, assuming isotropic rotation (eq 1, using 71.6 G for the rigid limit value, $2T_{\parallel}$). To determine whether the labeled RLC is immobilized on myosin heads, we reincorporated labeled RLC into RLC-extracted scallop myofibrils. The EPR spectrum of these myofibrils in rigor (Figure 2, middle) showed a much wider splitting ($2T_{\parallel}' = 71.4 \pm 0.1$ G) than that of labeled RLC in solution. Immobilization of labeled RLC on glass beads (spectrum not shown) produced essentially the same splitting (the rigid limit value of $2T_{\parallel} = 71.6 \pm 0.1$ G), indicating that there is no nanosecond motion of the spin labels when the RLC is bound to the myosin heads. This is the first LC probe to be shown to be so strongly immobilized (*29, 30*), indicating that its ST-EPR spectra are a reliable indicator of the microsecond rotational motion of the LC domain. The ST-EPR spectrum of InVSL-RLC myofibrils in rigor (Figure 2, bottom) has a line shape approaching but not quite reaching that of the rigid limit, indicating an effective rotational correlation time of 160 ± 30 μs (*27*).

EPR Spectra of RLC-Labeled Scallop Fiber Bundles. The conventional EPR spectrum of spin-labeled *Mercenaria* RLC in scallop fibers in rigor, oriented perpendicular to the

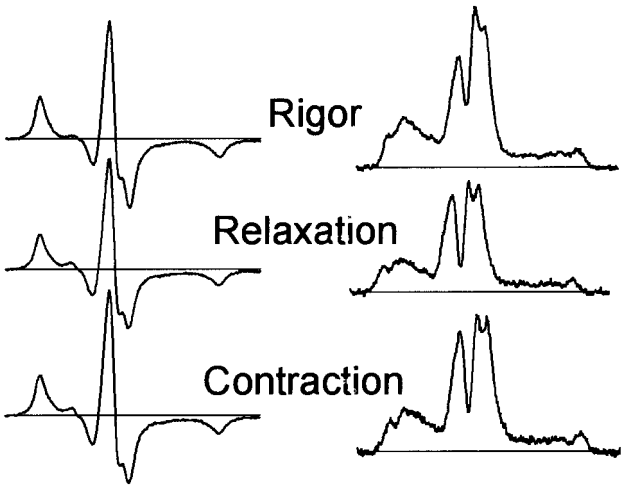

FIGURE 3: Conventional (left column) and ST-EPR (right column) spectra of InVSL-RLC in scallop muscle fiber bundles aligned perpendicular to the magnetic field in rigor solution (top), relaxation solution (middle), and contraction solution (bottom). Each spectrum has been normalized to unit concentration before plotting.

magnetic field (Figure 3, top left), is virtually indistinguishable from that of randomly oriented myofibrils (Figure 2, center) or from that of fibers oriented parallel to the field (not shown). Essentially identical conventional EPR spectra were observed in rigor, relaxation, and contraction, indicating disorder but no nanosecond motion (Figure 3, left column). Thus the spin labels are disordered with respect to the muscle fiber axis, preventing measurements of orientational changes of the LC domain. The lack of orientational dependence, coupled with the strong probe immobilization on the LC, provides an advantage for the measurement of microsecond rotational motion by ST-EPR spectroscopy. The changes in the ST-EPR spectrum will unambiguously be due to microsecond rotational motions of the LC domain, not to orientational changes.

Rotational Motions of Labeled RLC in Scallop Fiber Bundles. Unlike the conventional EPR spectra (Figure 3, left), the ST-EPR spectra of scallop fibers in rigor, relaxation, and contraction (Figure 3, right column) show clear differences in the spectral line shapes, particularly in the low- and mid-field regions, indicating distinct differences in microsecond rotational motions. The effective rotational correlation time is maximal (indicating minimal rotational mobility) in rigor ($\tau_r^{eff} = 140 \pm 5$ μs), minimal in relaxation ($\tau_r^{eff} = 70 \pm 4$ μs), and intermediate in contraction ($\tau_r^{eff} = 100 \pm 5$ μs) (Table 2). We found that the spectrum in contraction was an excellent fit to a linear combination of the spectra in rigor and relaxation (eq 2). The best fit (minimum χ^2) was for $X_{RIG} = 0.65 \pm 0.04$ (SEM, $n = 5$), consistent with a model in which 35% of the myosin heads in contraction have the same low mobility as in rigor, while 65% have the same higher mobility as in relaxation.

Direct Effects of Divalent Cation Binding to RLC. For spin-labeled RLC in solution, Mg has a slight immobilizing effect on the spin label in metal-free RLC, and the further addition of Ca (final free $[Ca^{2+}] = 10$ μM) to Mg-bound RLC in solution has a slight additional immobilizing effect (Table 3). This Ca effect is reversed on removal of Ca by dialysis. This indicates that Ca replaces Mg on the RLC under these conditions, resulting in a slight decrease in probe rotational mobility. However, this Ca-binding perturbation occurs in fibers only when ATP is present. In the absence of ATP (in rigor), the conventional and ST-EPR spectra of the scallop fiber bundles with bound Mg are unchanged by the addition of Ca, indicating that the rotational mobility of labeled RLC is not perturbed by Ca binding or that Ca does not significantly replace bound Mg when the RLC is bound to the heavy chain. It was previously shown that the rate of dissociation of Mg from RLC is slower (0.05 s^{-1}) than Ca activation of scallop muscle (*42*). We conclude that the effect observed when Ca is added to relaxation (Table 2) is due to a structural change involved in muscle activation (which involves Ca binding to the specific Ca binding site in ELC−RLC), not to a localized change due to Ca binding to the nonspecific divalent cation site in RLC.

Table 2: Spectral Parameters and τ_r^{eff} for Labeled RLC on Scallop Fibers in Rigor, Relaxation, and Contraction[a]

	L''/L	τ_r^{eff} (μs)	X_{RIG}
rigor	1.30 ± 0.01	140 ± 5	1.0
relaxation	0.98 ± 0.02	70 ± 4	0
contraction	1.14 ± 0.01	100 ± 5	0.35 ± 0.08
rigor + Ca	1.32 ± 0.05	143 ± 10	1.0 ± 0.1

[a] The L''/L parameter (Figure 2, third spectrum) was determined from a ratio of spectral heights in the low-field region of the ST-EPR as described by Roopnarine et al. (*27*). τ_r^{eff} was determined from standard plots for L''/L vs τ_r as described in Roopnarine et al. (*27*). X_{RIG} is the fraction of rigor-like component determined from simulated composite spectra assuming a linear combination of end-point spectra as described in Materials and Methods. Reported values are mean ± SEM for $n = 5$.

Table 3: Effect of Divalent Cation on the Conventional EPR Spectra of RLC in Solution[a]

divalent cation	splitting (G)	τ_r^{eff} (ns)
no divalent cation	62.6 ± 0.1	9.0 ± 0.2
2 mM Mg	63.2 ± 0.1	10.4 ± 0.2
2 mM Mg + 10 μM Ca	63.8 ± 0.1	11.1 ± 0.2

[a] Divalent cations were in NaN_3 wash as defined in Materials and Methods. Splitting in gauss (G) was measured between the outer extrema of the EPR spectra. τ_r^{eff} is the effective rotational correlation time, calculated with eq 1. Reported values are mean ± SEM for $n = 5$.

DISCUSSION

Labeled RLC Is Functionally Incorporated. A significant advantage of molluscan muscle, compared with vertebrate muscle, is the relative ease of complete RLC extraction and the clear demonstration of specific functional (Ca-sensitive MgATPase) incorporation of labeled RLC (Figure 1, Table 1), as shown previously in scallop muscle for unlabeled scallop RLC (*17*, *43*) and unlabeled *Mercenaria* RLC (*19*). The mechanical properties of scallop fiber bundles were also restored with the rebinding of labeled RLC, as shown previously for unlabeled RLC (*33*, *34*). The observation of normal Ca-sensitive function after spin-labeling Cys 51 is consistent with similar observations after modification of this and other Cys in molluscan RLC (*28*, *31*, *44*−*46*). Our results clearly show that virtually all of the myosin in the scallop fiber bundles contained InVSL-labeled *Mercenaria* RLC and had biochemical and mechanical properties identical to those of native myosin, because the labeled RLC were functionally bound to myosin. None of these goals has been so clearly achieved in studies of vertebrate skeletal muscle,

where complete RLC extraction has not been achieved and where functional effects of RLC reincorporation are much more subtle (*22*, *23*, *47*, *48*).

Interpretation of Conventional EPR Spectra. The study of the rotational dynamics of myosin during force generation requires that the spin label be strongly immobilized on the protein (*27*). The spin label InVSL has consistently resulted in strong immobilization on both muscle (*27*) and membrane proteins (*49*). We have consistently observed wider splittings ($2T_{\parallel}'$) with InVSL than with other spin labels attached to either RLC (*26*, *29*, *30*) or SH1 on the myosin heavy chain (*27*). The strongly immobilized population on InVSL-RLC has a splitting of 62.6 ± 0.1 G, which is wider than that previously observed with MSL or IASL at the same site (*28*, *31*), suggesting that InVSL is more strongly immobilized on RLC than the other spin labels. In fact, this splitting yields an effective rotational correlation time of 9 ns, which is the value expected for the rigid-body rotational diffusion of the RLC, consistent with rigid binding of the probe. Immobilization of the labeled RLC on myofibrils or glass beads eliminated the weakly immobilized component (Figure 2), suggesting either rigidification of the RLC structure or direct steric interaction with the spin label. For the remaining strongly immobilized component, the splitting increased to the rigid-limit value (71.4 ± 0.1 and 71.6 ± 0.1 G, respectively), implying the elimination of nanosecond motion, confirming that the probe is rigidly bound to the protein. Thus the ST-EPR spectra of these samples can be reliably interpreted in terms of microsecond (or slower) rotational motion of the RLC and the LC domain.

Conventional EPR spectra of InVSL−RLC on scallop fiber bundles in rigor, relaxation, and contraction (Figure 3, left column) are typical of highly disordered spin labels, with the full width of angular distribution greater than 90° (*3*). The similarity of the spectra (wide peak-to-peak splitting, indicating strong immobilization) in the different physiological states indicates that no nanosecond rotational motion of InVSL-RLC is induced by ATP or Ca. The high degree of disorder, in contrast to the precise orientational order observed for the same spin label bound to SH1 (Cys 707) on the catalytic domain of rabbit skeletal muscle (*37*), could not be due to improper binding of the RLC to the heavy chain, since *Mercenaria* RLC restores functional properties of scallop myosin and muscle fibers. In addition, it has been previously shown to bind to the heavy chain more strongly than native scallop RLC even when labeled at Cys 51 (*19*, *42*). Our observation that LC-bound probes are more orientationally disordered than probes on the catalytic domain is consistent with electron microscopic (*50*) and EPR (*22*) studies suggesting that the distal (LC) domains of myosin heads in a two-headed cross-bridge are less uniformly oriented than the domains bound to actin (catalytic domains) and that this disorder in the LC domain is exacerbated by the helical mismatch of thick and thin filaments (*22*, *51*). The crystal structure of S1 shows flexible heavy chain protein loops flanking the LC domain (*11*, *12*), suggesting that considerable disorder (e.g., bending about hinges) could occur even when the catalytic domain is stereospecifically bound to actin. However, the extent of spin label disorder evident in our spectra (Figure 3, left) is greater than that observed in other spectroscopic studies of light chains in muscle fibers (*22*−*25*, *48*), including scallop muscle (*26*). Therefore, much of the disorder observed by EPR in the present study is probably due to the failure of the spin label, despite its site-specific labeling and strong immobilization, to find a single stereospecific conformation on the labeled RLC. Although this probe disorder prevents us from using this spin label to determine the orientation of the labeled RLC, the combination of probe disorder and strong immobilization establishes ideal conditions for the measurement of microsecond rotational motions of the LC domain, using ST-EPR; i.e., a change in the ST-EPR spectrum cannot be due to a change in probe orientation or nanosecond dynamics but must be due to a change in microsecond dynamics, which probably corresponds to global motion of the LC domain.

Interpretation of ST-EPR Spectra. Analysis of ST-EPR of fibers in rigor (Figure 3, right column) shows that τ_r^{eff} is 140 ± 5 μs (Table 2), and relaxation causes a 2-fold increase in rotational mobility (τ_r^{eff} = 70 ± 5 μs) (Table 2). This ATP-induced increase in rotational mobility during relaxation suggests that changes in structural dynamics are translocated from the catalytic domain to the LC domain. Alternatively, the rotational motions observed during relaxation may reflect rotation about a flexible site within myosin, as a result of the myosin head's detachment from actin. Ca activation during relaxation induces slower rotational motions, presumably inducing strong actin attachment of myosin heads during force generation. The effective rotational correlation time during contraction is intermediate between rigor and relaxation (τ_r^{eff} = 100 ± 5 μs). The effect of Ca in the absence of nucleotides was negligible (Table 2), consistent with previous observations that Ca-induced structural changes occur only when the nucleotide site is occupied (*26*, *44*).

The increases in effective correlation times (τ_r^{eff}) from relaxation (70 μs) to contraction (100 μs) to rigor (140 μs) could be modeled to reflect increases in the actual correlation times (τ_r, the time needed for the Brownian rotation of about 1 rad) and/or decreases in the amplitudes of rotational motion ($\Delta\theta$, full width), as shown by previous theoretical EPR simulations (*41*). If the amplitude of motion is less than 30°, then the actual correlation times could be much less than those estimated (*41*). However, the angular disorder of probes in the present study is much greater than 30°, suggesting that the estimated correlation times are accurate (*41*).

An alternative model, suggested by the observation that the spectrum in contraction is intermediate between those in relaxation and rigor, is to assume that contraction is a linear combination of the other two states. This model fits the data well, with the best fit giving a 35% contribution from the spectrum in rigor (Table 2). However, ST-EPR does not resolve motions with different correlation times in the microsecond time range (*41*), so this model is no more valid than the above analysis assuming a single correlation time.

Comparison with Catalytic Domain Dynamics. All previous ST-EPR studies of myosin head rotational dynamics in muscle fibers have involved probes attached to the catalytic domain in rabbit skeletal muscle. An ST-EPR study of spin labels attached to the catalytic domain in scallop myosin and S1 (*52*) showed similar rotational motions similar to those of skeletal myosin and S1 (*53*, *27*), so it is reasonable to compare ST-EPR of rabbit psoas muscle fibers with that of scallop muscle fibers, to gain insight into relative motions

of the catalytic and LC domains. The very low rotational mobility of spin-labeled LC domain in rigor (Figure 3, Table 2) matches that observed previously for the same spin label bound to Cys 707 on the catalytic domain (*27*). *We conclude that the two domains of the myosin head are essentially fixed relative to each other in rigor muscle.* The addition of ATP (relaxation) produces qualitatively similar increases in rotational mobility of the two domains, with intermediate mobility upon subsequent addition of Ca (contraction) (ref *3* and Table 2), suggesting that *force generation corresponds to a transition from dynamic disorder to order in both domains of the myosin head (2, 3, 5*−*7, 54, 55*). However, ATP increases rotational motion much more for the catalytic than the LC domain: In relaxation, InVSL on the catalytic domain is 7 times as mobile [$\tau_r^{eff} = 10$ μs (*3*)] as observed for the same spin label on the LC domain ($\tau_r^{eff} = 70$ μs, Table 2). Similarly, during contraction, catalytic domain mobility is twice as great [$\tau_r^{eff} = 50$ μs *(3)*] as in the LC domain (100 μs, Table 2). Thus, while the motions of InVSL are similarly restricted on the two domains in rigor (when actin and the myosin filament backbone combine to keep the two domains relatively fixed), *the rotational mobility of the LC domain is less than that of the catalytic domain during relaxation and contraction*, when actin no longer completely restricts the catalytic domain but the myosin filament backbone still partially restricts LC mobility. This is consistent with ST-EPR of spin labels attached to LC domains in isolated myosin filaments (*56*). These results strongly suggests *flexibility of the myosin head, such that the catalytic and LC domains rotate relative to each other*.

Relationship to Structural Studies. X-ray diffraction (*57*) and electron microscopic (*58*) studies indicate that cross-bridge helical order is maximal in relaxation. Thus the maximal rotational dynamics we observe in relaxation must correspond primarily to domain rotations within the cross-bridge that do not destroy helical order of the cross-bridge array. A similar conclusion was reached in coordinated electron microscopy and EPR studies of insect flight muscle (*59*). The combination of decreased microsecond mobility and decreased helical order upon muscle activation is probably due to cross-bridges that become immobilized on actin, which have helical mismatch with respect to myosin.

Relationship to Previous Spectroscopic Studies. The present results are consistent with a previous study of phosphorescent probes on gizzard RLC in scallop muscle, showing microsecond-time-range rotational motion in contraction that is intermediate between that of relaxation and rigor (6). The low orientational order of probes in the present study is an advantage for the analysis of ST-EPR spectra, since any changes in spectra must be due to changes in rotational motion, not orientation. However, ST-EPR lacks time resolution, so it does not provide direct information about the number of distinct probe populations that are present. In conventional EPR studies of spin-labeled RLC in rabbit muscle (*22, 23, 48*), the spin labels were not sufficiently immobilized and oriented to reveal distinct angles in relaxation or contraction. Fluorescence polarization has also failed to detect distinct angles of the LC domain (*24, 25*), probably because fluorescence lacks the required orientational resolution.

However, in a recent study of the orientational distribution of spin labels on the LC domain in scallop muscle, using an FDNA spin label attached to Cys 108 on chicken gizzard RLC, the probes were much better oriented than in the present study (and in any other study), permitting a high-resolution analysis of the orientational distribution in terms of multiple populations (*26*). It was shown that the orientational distribution in all three physiological states is a linear combination of the same two distinct orientational populations, which differ in their central angles by 36°± 5°. Since relaxation, contraction, and rigor corresponded to 50% ± 2%, 67% ± 3%, and 92% ± 2% of the second angular population (designated M2), respectively (*26*), it follows that the orientational distribution in contraction was a linear combination of that in relaxation (60% ± 4%) and rigor (40% ± 4%). Our results in the present study are consistent with those results, since the spectrum in contraction is a good fit to a linear combination of the spectra obtained in relaxation (65% ± 4%) and rigor (35% ± 8%) (Table 2). We conclude that the LC domain orientational populations in the study of Baker et al. (*26*) probably correspond to motional populations in the present study, even though those motional populations are not spectrally resolved by ST-EPR. If we assume that the M2 population (centered at 38°) always has the same low rotational mobility that it has in rigor (effective correlation time 140 μs from the present study), we can obtain the ST-EPR spectrum of the M1 population (centered at 74°) in relaxation by subtracting half of the rigor spectrum from the relaxation spectrum. This produces a spectrum (not shown) corresponding to an effective rotational correlation time of 42 μs, substantially shorter than the 70 μs effective (average) correlation time in relaxation.

In summary, when we combine the data in the present study with those of Baker et al. (*26*), we arrive at a model (Figure 4) in which the myosin LC domain has two structural (orientational) states (M1 and M2) differing in their mean orientation by 36°. Each of these states has some dynamic disorder, characterized by rotational correlation times of 42 μs (M1) and 140 μs (M2). Force generation involves a transition, in about $^1/_3$ of the heads from a weak-binding state, in which these structural states are equally populated, to a strong-binding state, in which only the less mobile (M2) structural state is populated (Figure 4). Alternatively, the

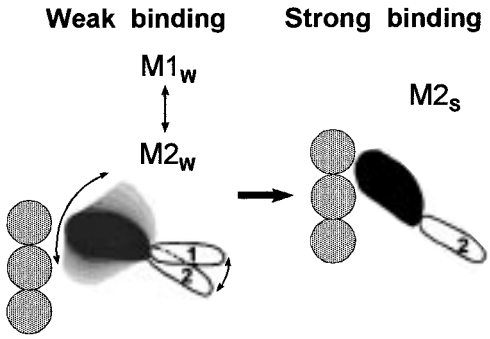

FIGURE 4: Model for the force-generating transition in muscle, in which the transition from weak (w) to strong (s) actin binding produces disorder-to-order transitions in both domains of the myosin head. In the weak-binding state, both domains are dynamically disordered, but the LC domain (white) is more ordered (less mobile) than the catalytic domain (black) and is equally distributed between two distinct orientational states (M1 and M2). Upon strong binding to actin (gray circles), both domains become more ordered (less mobile), with only one of the two LC domain states (M2) being significantly populated. Both domain movements contribute to actin movement and force.

shorter apparent correlation time we observe in relaxation (70 μs) could indicate the time scale of interconversion of the M1 and M2 structural states in relaxation.

Model of Force Generation. Figure 4 illustrates a model for the force-generating step in muscle contraction that is suggested by the present study and by previous EPR studies. In this model, the weak-binding (pre-force, mainly detached from actin) state is characterized by microsecond dynamic disorder of myosin heads (Figure 4, left), and force involves an ordering of the heads to a final strong-binding state that is rigid and more tilted (Figure 4, right). The disorder-to-order transition in the catalytic domain is clearly supported by spectroscopy (*3*−*6*) and electron microscopy (*60*). The present study and that of Baker et al. (*26*) show that the LC domain (in white, Figure 4) also undergoes this disorder-to-order transition, but it is more ordered and less mobile than the catalytic domain (in black, Figure 4) in the weak-binding state, so that two distinct orientations of the LC domain are resolvable and are equally populated (defined as M1 and M2 in ref *26* and Figure 4). The lower rotational mobility of the LC domain relative to the catalytic domain in the weak-binding state is probably due to the LC domain's association with the thick filament backbone. These two distinct orientations in weak-binding states are also consistent with electron microscopic analysis of scallop myosin filaments (*61*). On strong binding to actin, both domains become more ordered (less mobile), with only one of the two LC domain states (M2) being significantly populated. Thus our results are consistent with a *disorder-to-order transition* in force generation (*3*−*6*), in which the *LC domain rotates relative to the catalytic domain*, as illustrated in Figure 4 (*9*−*11*, *24*, *26*, *62*, *63*).

Conclusions. This is the first ST-EPR study of LC dynamics in muscle fiber bundles. The spin label, bound to Cys 51 on the RLC, undergoes only slight rotational motion on the submillisecond time scale in rigor. Relaxation with ATP increases the rotational motion, while in contraction (ATP plus Ca) the rotational motion is intermediate between relaxation and rigor, indicating that activation of contraction by Ca restricts the rotational motion of the LC domain. These changes in rotational motion are qualitatively similar to, but quantitatively different from, those observed previously for the same spin label on the catalytic domain. These results support a model for force generation involving rotational motion of the LC domain relative to the catalytic domain, and dynamic disorder-to-order transitions in both domains.

ACKNOWLEDGMENT

We thank Nicholas J. Meyer for assistance in tension measurements. We also thank Roberta L. H. Bennett for development of EPR data analysis software and spectrometer maintenance, and Nicoleta Cornea for development and maintenance of computational hardware and software. All of the above are affiliated with the University of Minnesota Medical School (Minneapolis, MN). We are especially indebted to Dr. Kálmán Hideg, from the University of Hungary at Pécs, for generously providing us with the spin label InVSL.

REFERENCES

1. Huxley, H. E. (1969) *Science 164*, 1356−1366.
2. Cooke, R., Crowder, M. S., and Thomas, D. D. (1982) *Nature 300*, 776−778.
3. Roopnarine, O., and Thomas, D. D. (1995) *Biophys. J. 68*, 1461−1471.
4. Berger, C. L., Svensson, E. C., and Thomas, D. D. (1989) *Proc. Natl. Acad. Sci. U.S.A. 86*, 8753−8757.
5. Berger, C. L., and Thomas, D. D. (1994) *Biophys. J. 67*, 250−261.
6. Thomas, D. D., Ramachandran, S., Roopnarine, O., Hayden, D. W., and Ostap, E. M. (1995) *Biophys. J. 68*, 135s−141s.
7. Roopnarine, O., and Thomas, D. D. (1996) *Biophys. J. 70*, 2795−2806.
8. Huxley, H. E., and Kress, M. (1985) *J. Muscle Res. Cell Motil. 6*, 153−161.
9. Cooke, R. (1986) *CRC Crit. Rev. Biochem. 21*, 53−118.
10. Rayment, I., Rypniewski, W. R., Schmidt-Bäse, K., Smith, R., Tomchick, D. R., Benning, M. M., Winklemann, D. A., Wesenberg, G., and Holden, H. M. (1993b) *Science 261*, 50−58.
11. Rayment, I., Holden, H. M., Whittaker, M., Yohn, C. B., Lorenz, M., Holmes, K. C., and Milligan, R. A. (1993) *Science 261* , 58−65.
12. Xie, X., Harrison, D. H., Schlichting, I., Sweet, R. M., Kalabokis, V. N., Szent-Györgyi, A. G., and Cohen, C. (1994) *Nature 368*, 306−312.
13. Fromherz, S., and Szent-Györgyi, A. G. (1995) *Proc. Natl. Acad. Sci. U.S.A. 92*, 7652−7653.
14. Jancso, A., and Szent-Györgyi, A. G. (1994) *Proc. Natl. Acad. Sci. U.S.A. 91*, 8762−8766.
15. Kalabokis, V. N., O'Neall-Hennessey, E., and Szent-Györgyi, A. G. (1994) *J. Muscle Res. Cell Motl. 15*, 546−553.
16. Chantler, P. D., and Szent-Györgyi, A. G. (1980) *J. Mol. Biol. 138*, 473−492.
17. Kendrick-Jones, J., Szentkiralyi, E. M., and Szent-Györgyi, A. G. (1976) *J. Mol. Biol. 104*, 747−775.
18. Simmons, R. M., and Szent-Györgyi, A. G. (1978) *Nature 273*, 62−64.
19. Sellers, J., Chantler, P. D., and Szent-Györgyi, A. G. (1980) *J. Mol. Biol. 144*, 223−245.
20. Persechini, A., Stull, J. T., and Cooke, R. (1985) *J. Biol. Chem. 260*, 7951−7954.
21. Lowey, S., Waller, G. S., and Trybus, K. M. (1993) *Nature 365*, 454−456.
22. Arata, T. (1990) *J. Mol. Biol. 214*, 471−478.
23. Hambly, B., Franks, K., and Cooke, R. (1992) *Biophys. J. 63*, 1306−1313.
24. Irving, M., Allen, T. St. C., Sabido-David, C., Craik, J. S., Brandmeier, B., Kendrick-Jones, J., Corrie, J. E. T., Trentham, D. R., and Goldman, Y. E. (1995) *Nature 375*, 688−691.
25. Ling, N., Shrimpton, C., Sleep, J., Kendrick-Jones, J., and Irving, M. (1996) *Biophys. J. 70*, 1836−1846.
26. Baker, J. E., Brust-Mascher, I., Ramachandran, S., and Thomas, D. D. (1998) *Proc. Natl. Acad. Sci. U.S.A. 95*, 2944−2949.
27. Roopnarine, O., Hideg, K., and Thomas, D. D. (1993) *Biophys. J. 64*, 1986−1907.
28. Chantler, P. D., and Szent-Györgyi, A. G. (1978) *Biochemistry 17*, 5440−5447.
29. Roopnarine, O., Szent-Györgyi, A. G., and Thomas, D. D. (1993) *Biophys. J. 64*, A231.
30. Roopnarine, O., Szent-Györgyi, A. G., and Thomas, D. D. (1995) *Biophys. J. 68*, 337s.
31. Bagshaw, C. R., and Kendrick-Jones, J. (1980) *J. Mol. Biol. 140*, 411−433.
32. Hankovszky, H. O., Hideg, K., and Jerkovich, G. (1989) *Synthesis 7*, 526−529.
33. Simmons, R. M., and Szent-Györgyi, A. G. (1980) *Nature 286*, 626−627.
34. Simmons, R. M., and Szent-Györgyi, A. G. (1985) *J. Physiol. 358*, 47−64.
35. Saraswat, L. D., and Lowey, S. (1991) *J. Biol. Chem. 266*, 19777−19785.
36. Thomas, D. D., and Cooke, R. (1980) *Biophys. J. 32*, 891−906.

37. Roopnarine, O., and Thomas, D. D. (1994) *Biophys J. 67*, 1634−1645.
38. Goldman, S. A., Bruno, G. V., and Freed, J. H. (1972) *J. Phys. Chem. 6*, 1858−1860.
39. McCalley, R. C., Shimsick, E. J., and McConnell, H. M. (1972) *Chem. Phys. Lett. 13*, 115−119.
40. Squier, T. C., and Thomas, D. D. (1986) *Biophys. J. 49*, 921−929.
41. Howard, E. C., Lindahl, K. M., Polnaszek, C. F., and Thomas, D. D. (1993) *Biophys. J. 64*, 581−593.
42. Bennett, A. J., and Bagshaw, C. R. (1986) *Biochem. J. 233*, 173−177.
43. Szent-Györgyi, A. G., Szentkiralyi, E. M., and Kendrick-Jones, J. (1973) *J. Mol. Biol. 74*, 179−203.
44. Hardwicke, P. M. D., Wallimann, T., and Szent-Györgyi, A. G. (1983) *Nature 201*, 478−482.
45. Hardwicke, P. M. D., and Szent-Györgyi, A. G. (1985) *J. Mol. Biol. 183*, 203-211.
46. Chantler, P. D., and Tao, T. (1986) *J. Mol. Biol. 192*, 87−99.
47. Szczesna, D., Zhao, J., and Potter, J. D. (1996) *J. Biol. Chem. 271*, 5246−5250.
48. Hambly, B., Franks, K., and Cooke, R. (1991) *Biophys. J. 59*, 127−138.
49. Horvath, L. I., Dux, L., Hankovszky, H. O., Hideg, K., and Marsh, D. (1992) *Biophys. J. 58*, 231−241.
50. Craig, R., Szent-Györgyi, A. G., Beese, L. A., Ficker, P., Vibert, P., and Cohen, C. (1980) *J. Mol. Biol. 140*, 35−55.
51. Vibert, P., and Craig, R. (1983) *J. Mol. Biol. 165*, 303−320.
52. Wells, C., and Bagshaw, C. R. (1983) *J. Mol. Biol. 164*, 137−157.
53. Thomas, D. D., Seidel, J. C., Hyde, J. S., and Gergely, J. (1975). *Proc. Natl. Acad. Sci. U.S.A. 72*, 1729−1733.
54. Barnett, V. A., and Thomas, D. D. (1989) *Biophys. J. 56*, 517−523.
55. Ostap, E. M., Barnett, V. A. and Thomas, D. D. (1995) *Biophys. J. 69*, 177−188.
56. Adhikari, B., Hideg, K., and Fajer, P. G. (1997) *Proc. Natl. Acad. Sci. U.S.A. 94*, 9643−9647.
57. Wray, J. S., Vibert, P. J., and Cohen, C. (1975) *Nature 257*, 561−564.
58. Vibert, P., and Craig R. (1985) *J. Cell Biol. 101*, 830−837.
59. Reedy, M. K., Lucaveche, C., Naber, N., and Cooke, R. (1992)- *J. Mol. Biol. 227*, 678−697.
60. Frado, L. L., and Craig, R. (1992) *J. Mol. Biol. 223*, 391−397.
61. Vibert, P. (1992) *J. Mol. Biol. 223*, 661−671.
62. Fisher, A. J., Smith, C. A., Thoden, J., Smith, R., Sutoh, K., Holden, H. M., and Rayment, I. (1995) *Biophys. J. 68*, 19s−28s.
63. Bershitsky, S. Y., Tsaturyan, A. K., Bershitskaya, O. N., Mashanov, G. I., Brown, P., Burns, R., and Ferenczi, M. A. (1997) *Nature 388*, 186−190.

BI9808363